



**Queensland University of Technology**  
Brisbane Australia

This is the author's version of a work that was submitted/accepted for publication in the following source:

Frost, Ray L. & Palmer, Sara J. (2011) Raman spectroscopy of stercorite  $\text{H}(\text{NH}_4)\text{Na}(\text{PO}_4) \cdot 4\text{H}_2\text{O}$  – a cave mineral from Petrogale Cave, Madura, Eucla, Western Australia. *Spectrochimica Acta Part A Molecular and Biomolecular Spectroscopy*, 79(5), pp. 1215-1219.

This file was downloaded from: <http://eprints.qut.edu.au/42533/>

© Copyright 2011 Elsevier B.V

**Notice:** *Changes introduced as a result of publishing processes such as copy-editing and formatting may not be reflected in this document. For a definitive version of this work, please refer to the published source:*

<http://dx.doi.org/10.1016/j.saa.2011.04.045>

**Raman spectroscopy of stercorite  $\text{H}(\text{NH}_4)\text{Na}(\text{PO}_4)\cdot 4\text{H}_2\text{O}$  – a cave mineral from  
Petrogale Cave, Madura, Eucla, Western Australia**

**Ray L. Frost<sup>\*</sup> and Sara J. Palmer**

Chemistry Discipline, Faculty of Science and Technology, Queensland University of  
Technology, GPO Box 2434, Brisbane Queensland 4001, Australia.

**ABSTRACT**

Raman spectroscopy complimented with infrared spectroscopy has been used to characterise the mineral stercorite  $\text{H}(\text{NH}_4)\text{Na}(\text{PO}_4)\cdot 4\text{H}_2\text{O}$ . The mineral stercorite originated from the Petrogale Cave, Madura, Eucla, Western Australia. This cave is one of many caves in the Nullarbor Plain in the South of Western Australia. These caves have been in existence for eons of time and have been dated at more than 550 million years old. The mineral is formed by the reaction of bat guano chemicals on calcite substrates. A single Raman band at  $920\text{ cm}^{-1}$  defines the presence of phosphate in the mineral. Antisymmetric stretching bands are observed in the infrared spectrum at 1052, 1097, 1135 and  $1173\text{ cm}^{-1}$ . Raman spectroscopy shows the mineral is based upon the phosphate anion and not the hydrogen phosphate anion. Raman and infrared bands are found and assigned to  $\text{PO}_4^{3-}$ ,  $\text{H}_2\text{O}$ , OH and NH stretching vibrations. The detection of stercorite by Raman spectroscopy shows that the mineral can be readily determined; as such the application of a portable Raman spectrometer in a ‘cave’ situation enables the detection of minerals, some of which may remain to be identified.

**KEYWORDS:** stercorite, ‘cave’ mineral, brushite, mundrabillaite, archerite, Raman spectroscopy.

---

<sup>\*</sup> Author to whom correspondence should be addressed (r.frost@qut.edu.au)

## 26 INTRODUCTION

27 The mineral stercorite originated from the Petrogale Cave, Madura, Eucla, Western Australia.  
28 As such, many minerals formed in these caves include archerite  $(\text{K},\text{NH}_4)(\text{H}_2\text{PO}_4)$  [1],  
29 mundrabillaite  $(\text{NH}_4)_2\text{Ca}(\text{HPO}_4)_2 \cdot \text{H}_2\text{O}$  [2]. These minerals occur as stalactites and as crusts  
30 on the walls and floors of the caves. Other minerals found in the Petrogale cave include  
31 aphthitalite  $(\text{K},\text{Na})_3\text{Na}(\text{SO}_4)_2$ , halite  $\text{NaCl}$ , syngenite  $(\text{K},\text{Na})_3\text{Na}(\text{SO}_4)_2$ , stercorite  
32  $\text{H}(\text{NH}_4)\text{Na}(\text{PO}_4) \cdot 4\text{H}_2\text{O}$ , oxammite  $(\text{NH}_4)_2(\text{C}_2\text{O}_4) \cdot \text{H}_2\text{O}$ , weddellite  $\text{Ca}(\text{C}_2\text{O}_4) \cdot 2\text{H}_2\text{O}$ ,  
33 whitlockite  $\text{Ca}_9\text{Mg}(\text{PO}_4)_6(\text{HPO}_4)$ , guanine  $\text{C}_5\text{H}_5\text{N}_5\text{O}$ , newberyite  $\text{Mg}(\text{HPO}_4) \cdot 3\text{H}_2\text{O}$  and calcite  
34  $\text{CaCO}_3$ . These minerals are formed through the chemical reactions of calcite with bat guano  
35 or with chemicals from bat guano which are water soluble and crystallise out on the calcite  
36 surfaces. The mineral stercorite is water soluble and may translocate through the Petrogale  
37 cave network [3].

38 The name ‘stercorite’ is derived from the Latin word for ‘dung’. Stercorite is a triclinic  
39 mineral (pseudomonoclinic) [4] and is whitish to yellow in colour. This mineral belongs to  
40 space group 1bar with cell dimensions  $a = 10.636(2)$   $b = 6.9187(14)$   $c = 6.4359(13)$   $\alpha =$   
41  $90.46(3)$   $\beta = 97.87(3)$   $\gamma = 109.20(3)$  with  $Z = 2$  [4]. The mineral is congruent with respect to  
42 its components. Stercorite has a (100) layered structure built up by [010] rows of Na  
43 octahedra sandwiched between P tetrahedra;  $\text{NH}_4^+$  and equivalent water molecules with  
44 tetrahedral environments, intercalate the layers and link them through H bonds [4]. The  
45 solubility and phase equilibrium diagram has been published [3].

46

The amount of published data on the Raman spectra of mineral phosphates is limited [5-9]. Further there is almost no data on the Raman spectroscopy of the phosphate ‘cave’ minerals. The Raman spectra of the hydrated hydroxy phosphate minerals have been reported only to a limited extent. In aqueous systems, Raman spectra of phosphate oxyanions show a symmetric stretching mode ( $\nu_1$ ) at  $938\text{ cm}^{-1}$ , the antisymmetric stretching mode ( $\nu_3$ ) at  $1017\text{ cm}^{-1}$ , the symmetric bending mode ( $\nu_2$ ) at  $420\text{ cm}^{-1}$  and the  $\nu_4$  bending mode at  $567\text{ cm}^{-1}$  [7, 8, 10]. More recent values have been reported by Rudolph and Irmner [11]. Density functional calculations enabled more precise measurements of the positions of the phosphate vibrational modes [11].

S.D. Ross in Farmer (1974) (page 404) listed some well-known minerals containing phosphate which were either hydrated or hydroxylated or both [12]. The value for the  $\nu_1$  symmetric stretching vibration of  $\text{PO}_4$  units was given as  $930\text{ cm}^{-1}$  (augelite),  $940\text{ cm}^{-1}$  (wavellite),  $970\text{ cm}^{-1}$  (rockbridgeite),  $995\text{ cm}^{-1}$  (dufrenite) and  $965\text{ cm}^{-1}$  (beraunite). The position of the symmetric stretching vibration is mineral dependent and a function of the cation and crystal structure. The fact that the symmetric stretching mode is observed in the infrared spectrum affirms a reduction in symmetry of the  $\text{PO}_4^{3-}$  units. This reduction in symmetry can be caused by site symmetry and/or factor group splitting.

Raman spectroscopy has proven most useful for the study of mineral structure [13-22]. The detailed comparative Raman spectra of the cave mineral stercorite have not been published. The objective of this research is to report the Raman and infrared spectra of stercorite and to relate the spectra to the mineral structure.

## **EXPERIMENTAL**

### **Mineral**

The mineral stercorite was supplied by The Australian Museum and originated from Petrogale Cave, Madura, Western Australia. Details of the mineral have been published (page 561) [23]. The mineral corresponds to the formula  $\text{H}(\text{NH}_4)\text{Na}(\text{PO}_4)\cdot 4\text{H}_2\text{O}$ .

### **Raman spectroscopy**

Crystals of stercorite were placed on a polished metal surface on the stage of an Olympus BSM microscope, which is equipped with 10x, 20x, and 50x objectives. The microscope is part of a Renishaw 1000 Raman microscope system, which also includes a monochromator, a filter system and a CCD detector (1024 pixels). The Raman spectra were excited by a Spectra-Physics model 127 He-Ne laser producing highly polarised light at 633 nm and collected at a nominal resolution of  $2\text{ cm}^{-1}$  and a precision of  $\pm 1\text{ cm}^{-1}$  in the range between 100 and  $4000\text{ cm}^{-1}$ . Repeated acquisition on the crystals using the highest magnification (50x) was accumulated to improve the signal to noise ratio in the spectra. Spectra were calibrated using the  $520.5\text{ cm}^{-1}$  line of a silicon wafer.

### **Infrared spectroscopy**

Infrared spectra were obtained using a Nicolet Nexus 870 FTIR spectrometer with a smart endurance single bounce diamond ATR cell. Spectra over the  $4000\text{--}525\text{ cm}^{-1}$  range were obtained by the co-addition of 128 scans with a resolution of  $4\text{ cm}^{-1}$  and a mirror velocity of  $0.6329\text{ cm/s}$ . Spectra were co-added to improve the signal to noise ratio.

Band component analysis was undertaken using the Jandel 'Peakfit' (Erkrath, Germany) software package which enabled the type of fitting function to be selected and allowed specific parameters to be fixed or varied accordingly. Band fitting was done using a Lorentz-Gauss cross-product function with the minimum number of component bands used for the fitting process. The Lorentz-Gauss ratio was maintained at values greater than 0.7 and fitting was undertaken until reproducible results were obtained with squared correlations ( $r^2$ ) greater than 0.995. Band fitting of the spectra is quite reliable providing there is some band separation or changes in the spectral profile.

## **RESULTS AND DISCUSSION**

The Raman spectrum of stercorite over the  $800\text{ to }1100\text{ cm}^{-1}$  and the infrared spectrum over the  $800\text{ to }1200\text{ cm}^{-1}$  range are displayed in Figs. 1a and 1b respectively. The complete Raman and infrared spectrum over the full wavenumber range is given in Fig. S1 in the supplementary information. A single band at  $920\text{ cm}^{-1}$  is observed in the Raman spectrum (Fig. 1a) and is assigned to the  $\nu_1\text{ PO}_4^{3-}$  symmetric stretching mode. The observation of a single band is perhaps unexpected, as with three different cations in the mineral structure, it

might be expected that the band would split into component bands. Further the single band observed in the Raman spectrum suggests that the symmetry of the phosphate anion is preserved in the mineral structure. In addition, the presence of the proton might suggest the existence of  $\text{HPO}_4^{2-}$  ions. If this is the case then again two symmetric phosphate stretching modes would be observed. This is not the case.

In the infrared spectrum (Fig. 1b) two low intensity bands at 989 and 1010  $\text{cm}^{-1}$  are attributed to this vibrational mode. An intense infrared band is found at 1097  $\text{cm}^{-1}$  with component bands at 1052, 1135 and 1173  $\text{cm}^{-1}$ . These bands are attributed to the  $\nu_3 \text{PO}_4^{3-}$  antisymmetric stretching mode. Raman bands in these positions were not observed. In the infrared spectrum, some low intensity bands are observed at 817, 871, 900 and 934  $\text{cm}^{-1}$ . The assignment of these bands have two possibilities: highly likely are water librational modes and secondly the band at 871  $\text{cm}^{-1}$  may be due to the symmetric stretching mode of  $\text{HPO}_4^{2-}$  units. However no bands in this position were observed in the Raman spectrum. This mitigates against this assignment.

The Raman spectrum over the 300 to 650  $\text{cm}^{-1}$  range and the infrared spectrum over the 550 to 800  $\text{cm}^{-1}$  range are displayed in Figs. 2a and 2b. Two Raman bands are resolved at 450 and 476  $\text{cm}^{-1}$  and are attributed to the  $\text{PO}_4^{3-} \nu_2$  bending mode. The observation of two bands suggests some distortion of the phosphate anion, perhaps brought about by the position of the different cations around the phosphate anion. The bands are not observed in the infrared spectrum as the position of the bands lies below the detection limit of the instrumentation. The two  $\nu_2$  infrared bands for pseudomalachite published by Farmer [12] were reported at 450 and 422  $\text{cm}^{-1}$ . For pseudomalachite Raman bands were observed at 482 and 452  $\text{cm}^{-1}$  with equal intensity. Cornetite Raman spectrum showed an intense band at 433  $\text{cm}^{-1}$  with minor components at 463 and 411  $\text{cm}^{-1}$ . Farmer [12] reported two bands at 464 and 411  $\text{cm}^{-1}$  for cornetite. Farmer [12] also reported a number of bands of phosphate minerals in the 480 to 680  $\text{cm}^{-1}$  region and ascribed these bands to the  $\nu_4$  modes. The intense infrared band at 615  $\text{cm}^{-1}$  with a shoulder on the low wavenumber side at 601  $\text{cm}^{-1}$  is attributed to the  $\nu_4$  vibrational modes. The Raman band at 577  $\text{cm}^{-1}$  may be the equivalent of this vibration observed in the infrared spectrum. The assignment of these bands is consistent with the data

reported by Farmer [12] in a series of Tables including Table 17. XV in which a wide range of hydrated divalent phosphates including the ammonium ion. In the infrared spectrum bands are observed at 755 and 773  $\text{cm}^{-1}$ . These bands are assigned to water librational modes. Raman bands observed at 326, 345 and 396  $\text{cm}^{-1}$  are considered to be related to the hydrogen bonding of the water to the phosphate units in the stercorite structure. The first two bands might be assigned to the  $\nu_2$  bending modes of the  $\text{PO}_4^{3-}$  ion.

The Raman spectrum over the 50 to 300  $\text{cm}^{-1}$  range and the infrared spectrum over the 1200 to 1800  $\text{cm}^{-1}$  range are displayed in Figs. 3a and 3b. Raman bands are observed at 110, 143, 155, 185, 197 and 216  $\text{cm}^{-1}$  and are simply described as lattice vibrations. The infrared peak centred upon 1631  $\text{cm}^{-1}$  is complex and a series of overlapping bands may be resolved. These bands are attributed to water HOH and ammonium HNH bending modes. The infrared bands at 1260, 1318, 1405 and 1443  $\text{cm}^{-1}$  are attributed to  $\text{NH}_4^+$  vibrations. Farmer tabulated  $\text{NH}_4^+$  vibrations in the 1410 to 1475  $\text{cm}^{-1}$  range for ammoniated divalent phosphates (Table 17. XV) and defined these bands as  $\text{NH}_4^+ \nu_4$  bending modes.

The Raman spectrum of stercorite over the 2700 to 3500  $\text{cm}^{-1}$  range and the infrared spectrum over the 2900 to 3700  $\text{cm}^{-1}$  range are displayed in Figs. 4a and 4b. Raman bands are observed at 2900, 3024 and 3158  $\text{cm}^{-1}$ . The first band is assigned to the NH stretching vibration of the  $\text{NH}_4^+$  units. The position of these bands suggests that the water is involved in strong hydrogen bonding. The latter two bands are due to water stretching vibrations. In the infrared spectrum four bands are observed at 3066, 3232, 3340 and 3578  $\text{cm}^{-1}$ . These bands are at higher wavenumbers than those in the Raman spectrum.

### **Mechanism of formation of stercorite**

In the laboratory, the mineral is readily synthesised by mixing aqueous solutions of sodium hydrogen phosphate  $\text{Na}_2\text{HPO}_4$  and ammonium hydrogen phosphate  $(\text{NH}_4)_2\text{HPO}_4$  [3]. Platford [3] showed that the two chemicals were in congruency with their components. It is likely that low temperatures aid the formation of stercorite, as might occur in caves on the

Nullarbor Plains in Western Australia. Whether or not the mineral stercorite is formed by simply solubility effects from undersaturated solutions is open to question, but it does seem likely. The presence of the calcite surface serves as a surface for the crystallisation of the stercorite.

## CONCLUSIONS

The mineral stercorite is an ammoniated hydrogen sodium phosphate and is found in caves in Western Australia and is especially known from the Petrogale Cave, near Madura, Western Australia. The mineral has also been found Ichaboe Island, Namibia and Gwãnape Island, Peru. It is a mineral formed by the reaction of calcite with bat (or bird) guano. The mineral is associated with other phosphate minerals including struvite, archerite, brushite. According to Platford [3], the mineral is formed from solution. Hence the basic components of the mineral can be translocated through a cave system.

The mineral because of the individual vibrating units, lends itself to vibrational spectroscopy. A combination of Raman and infrared spectroscopy has been used to identify vibrational modes associated with the mineral stercorite. The question arises as to whether the mineral contains hydrogen phosphate units or simply phosphate units. Based upon Raman spectroscopy the anion in the mineral is the phosphate anion and no observation of hydrogen phosphate units were found. The detection of stercorite by Raman spectroscopy shows that the mineral can be readily determined; as such the application of a portable Raman spectrometer in a 'cave' situation enables the detection of minerals in cave systems, some of which remain to be identified.

## Acknowledgments

The financial and infra-structure support of the Queensland University of Technology, Chemistry discipline is gratefully acknowledged. The Australian Research Council (ARC) is thanked for funding the instrumentation.



## 195 REFERENCES

- 196 [1] P.J. Bridge, Mineralogical Magazine, 41 (1977) 33-35.
- 197 [2] P.J. Bridge, R.M. Clark, Mineralogical Magazine, 47 (1983) 80-81.
- 198 [3] R.F. Platford, Journal of Chemical and Engineering Data, 19 (1974) 166-168.
- 199 [4] G. Ferraris, M. Franchini Angela, Acta Crystallographica, Section B: Structural
- 200 Crystallography and Crystal Chemistry, 30 (1974) 504-510.
- 201 [5] R.L. Frost, L. Duong, W. Martens, Neues Jahrbuch fuer Mineralogie, Monatshefte, (2003)
- 202 223-240.
- 203 [6] R.L. Frost, W. Martens, P.A. Williams, J.T. Klopogge, Journal of Raman Spectroscopy,
- 204 34 (2003) 751-759.
- 205 [7] R.L. Frost, W. Martens, P.A. Williams, J.T. Klopogge, Mineralogical Magazine, 66
- 206 (2002) 1063-1073.
- 207 [8] R.L. Frost, P.A. Williams, W. Martens, J.T. Klopogge, P. Leverett, Journal of Raman
- 208 Spectroscopy, 33 (2002) 260-263.
- 209 [9] R.L. Frost, P.A. Williams, W. Martens, J.T. Klopogge, Journal of Raman Spectroscopy,
- 210 33 (2002) 752-757.
- 211 [10] R.L. Frost, W.N. Martens, T. Klopogge, P.A. Williams, Neues Jahrbuch fuer
- 212 Mineralogie, Monatshefte, (2002) 481-496.
- 213 [11] W.W. Rudolph, G. Irmer, Applied Spectroscopy, 61 (2007) 1312-1327.
- 214 [12] V.C. Farmer, Mineralogical Society Monograph 4: The Infrared Spectra of Minerals,
- 215 1974.
- 216 [13] R.L. Frost, S. Bahfenne, J. Raman Spectrosc., 42 (2011) 219-223.
- 217 [14] R.L. Frost, S. Bahfenne, J. Cejka, J. Sejkora, J. Plasil, S.J. Palmer, E.C. Keefe, I.
- 218 Nemec, J. Raman Spectrosc., 42 (2011) 56-61.
- 219 [15] R.L. Frost, J. Cejka, J. Sejkora, J. Plasil, B.J. Reddy, E.C. Keefe, Spectrochim. Acta,
- 220 Part A, 78 (2011) 494-496.
- 221 [16] R.L. Frost, S.J. Palmer, Spectrochim. Acta, Part A, 78 (2011) 248-252.
- 222 [17] R.L. Frost, S.J. Palmer, Spectrochim. Acta, Part A, 78 (2011) 1255-1260.
- 223 [18] R.L. Frost, S.J. Palmer, Spectrochim. Acta, Part A, 78 (2011) 1250-1254.
- 224 [19] R.L. Frost, S.J. Palmer, S. Bahfenne, Spectrochim. Acta, Part A, 78 (2011) 1302-1304.
- 225 [20] R.L. Frost, B.J. Reddy, S.J. Palmer, E.C. Keefe, Spectrochim. Acta, Part A, 78 (2011)
- 226 996-1003.
- 227 [21] S.L. Reddy, K.S. Maheswaramma, R.R. Reddy, A.V. Reddy, Y. Nakamura, B.J. Reddy,
- 228 T. Endo, R.L. Frost, Spectrochim. Acta, Part A, 78 (2011) 1240-1244.
- 229 [22] J. Yang, H. Cheng, R.L. Frost, Spectrochim. Acta, Part A, 78 (2011) 420-428.
- 230 [23] J.W. Anthony, R.A. Bideaux, K.W. Bladh, M.C. Nichols, Handbook of Mineralogy
- 231 Vol.IV. Arsenates, phosphates, vanadates - Mineral Data Publishing, Tucson, Arizona,
- 232 Mineral data Publishing, Tucson, Arizona, 2000.

237 **List of Figures**

238 **Figure 1 (a) Raman spectrum of stercorite in the 800 to 1100 cm<sup>-1</sup> range and (b) infrared**  
239 **spectrum of stercorite in the 800 to 1200 cm<sup>-1</sup> range**

240

241 **Figure 2 (a) Raman spectrum of stercorite in the 300 to 650 cm<sup>-1</sup> range and (b) infrared**  
242 **spectrum of stercorite in the 550 to 800 cm<sup>-1</sup> range**

243

244 **Figure 3 (a) Raman spectrum of stercorite in the 50 to 300 cm<sup>-1</sup> range and (b) infrared**  
245 **spectrum of stercorite in the 1200 to 1800 cm<sup>-1</sup> range**

246

247 **Figure 4 (a) Raman spectrum of stercorite in the 2700 to 3500 cm<sup>-1</sup> range and (b)**  
248 **infrared spectrum of stercorite in the 2900 to 3700 cm<sup>-1</sup> range**

249

250

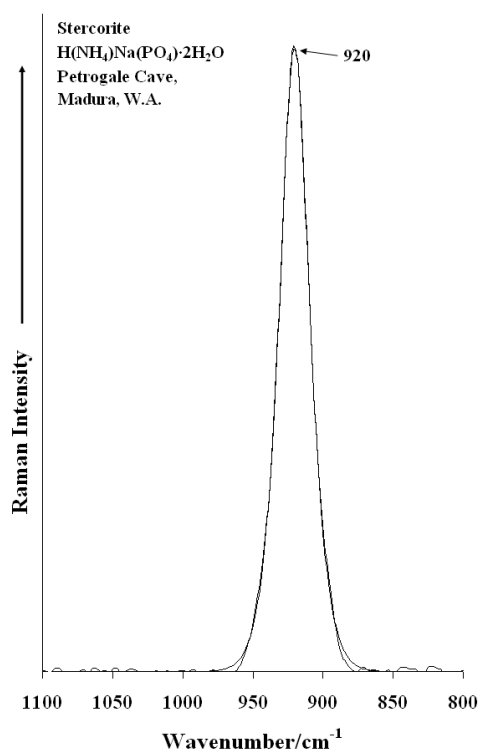


Fig.1a

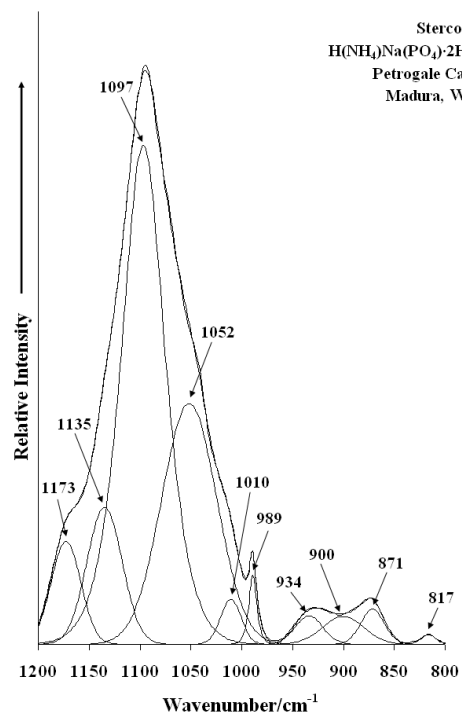


Fig.1b

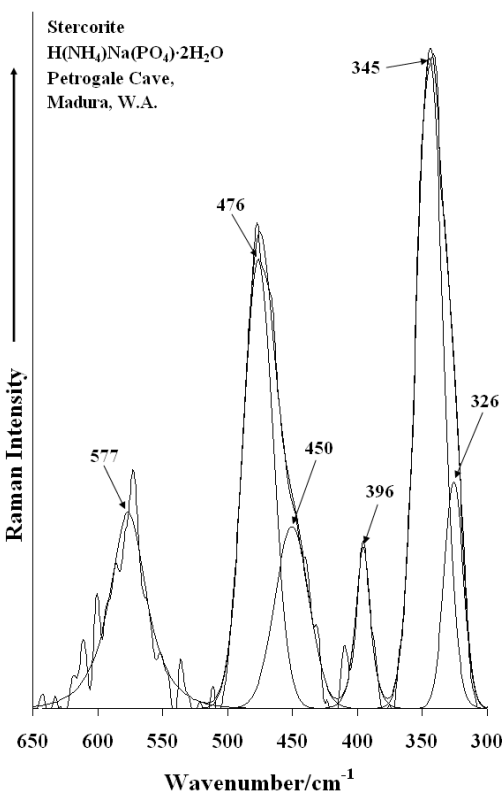


Fig. 2a

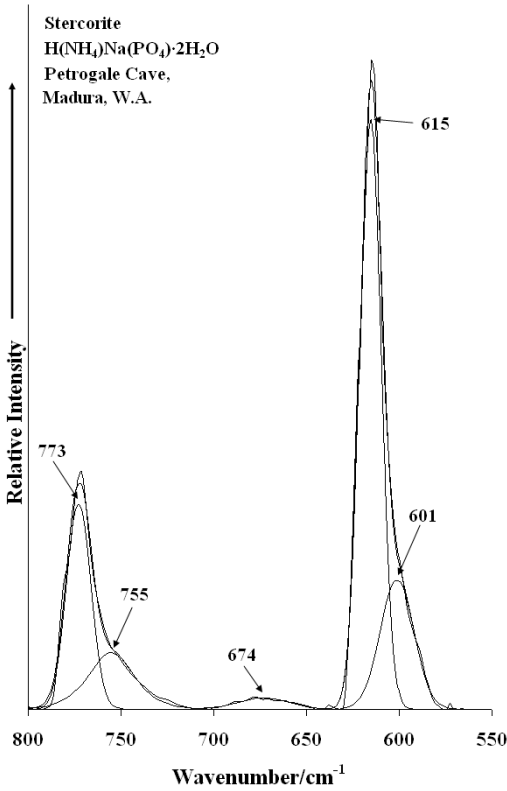


Fig. 2b

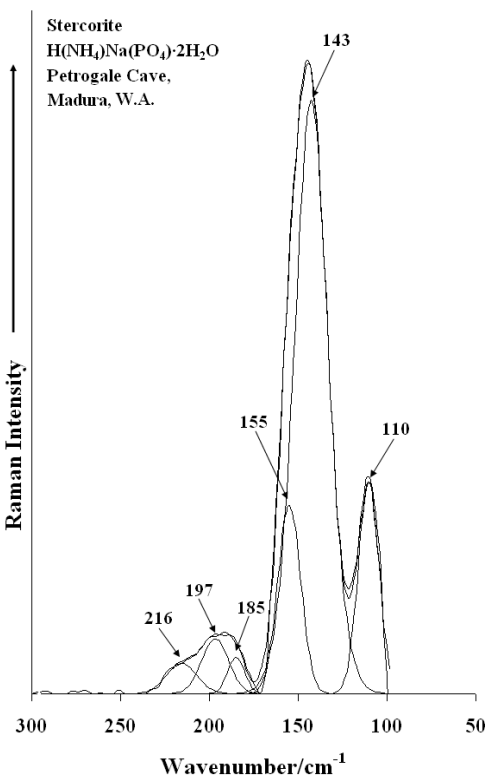


Fig. 3a

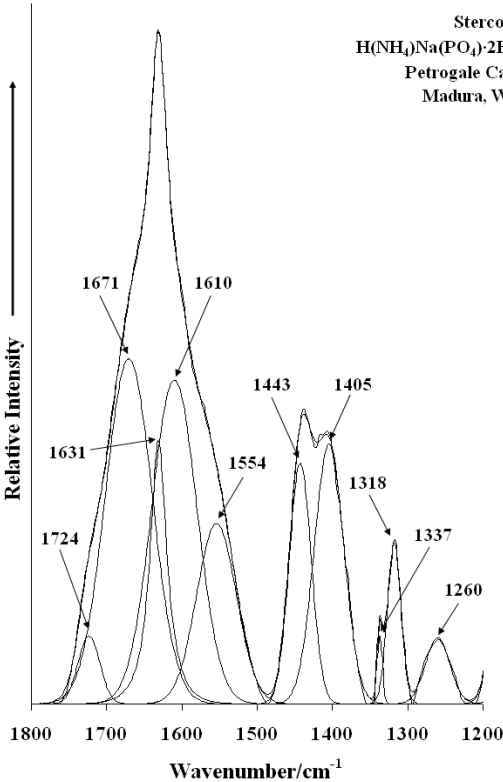


Fig. 3b

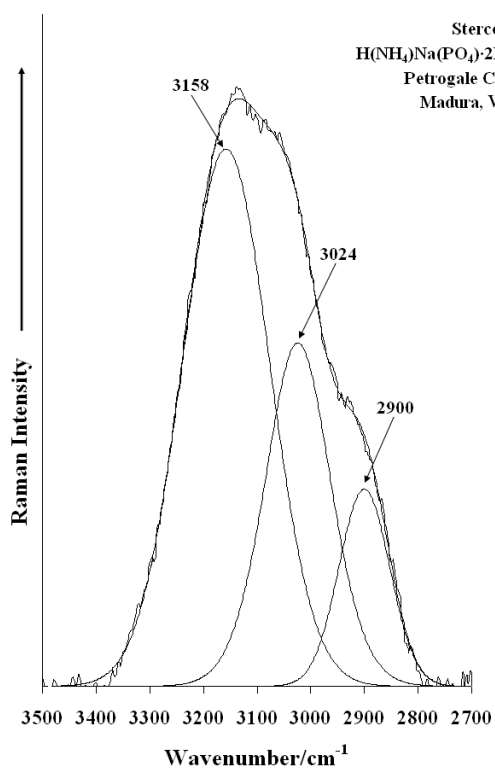


Fig. 4a

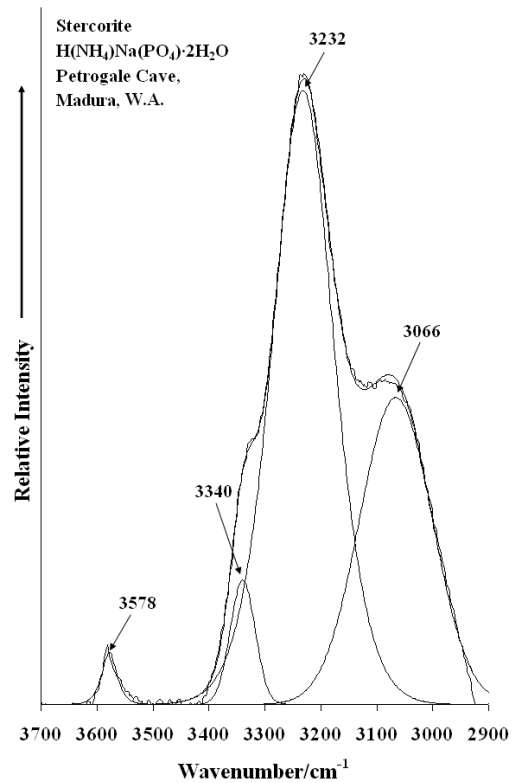


Fig. 4b